ACS Medicinal Chemistry Letters

Letter

pubs.acs.org/acsmedchemlett

Exploring Heteroaryl-pyrazole Carboxylic Acids as Human Carbonic Anhydrase XII Inhibitors

Roberta Cadoni,[†,▽] Nicolino Pala,[†,▽] Carrie Lomelino,[‡] Brian P. Mahon,[‡] Robert McKenna,[‡] Roberto Dallocchio,[§] Alessandro Dessì,[§] Mauro Carcelli,[∥] Dominga Rogolino,[∥] Vanna Sanna,[†] Mauro Rassu,[⊥] Ciro Iaccarino,[⊥] Daniela Vullo,[#] Claudiu T. Supuran,*[,#] and Mario Sechi*[,†]

[†]Department of Chemistry and Pharmacy, University of Sassari, Via Vienna 2, 07100 Sassari, Italy

[‡]Department of Biochemistry and Molecular Biology, College of Medicine, University of Florida, 1600 SW Archer Road, PO Box 100245, Gainesville, Florida 32610, United States

[§]Istituto CNR di Chimica Biomolecolare, Traversa La Crucca 3, 07100 Sassari, Italy

[∥]Department of Chemical, Life Science and Environmental Sustainability, University of Parma, Parco Area delle Scienze 17/A, 43124 Parma, Italy

[⊥]Department of Biomedical Sciences, University of Sassari, Via Muroni 25, 07100 Sassari, Italy

[#]Polo Scientifico, Neurofarba Department and Laboratorio di Chimica Bioinorganica, Università degli Studi di Firenze, Room 188, Via della Lastruccia 3, 50019 Sesto Fiorentino, Florence, Italy

Supporting Information

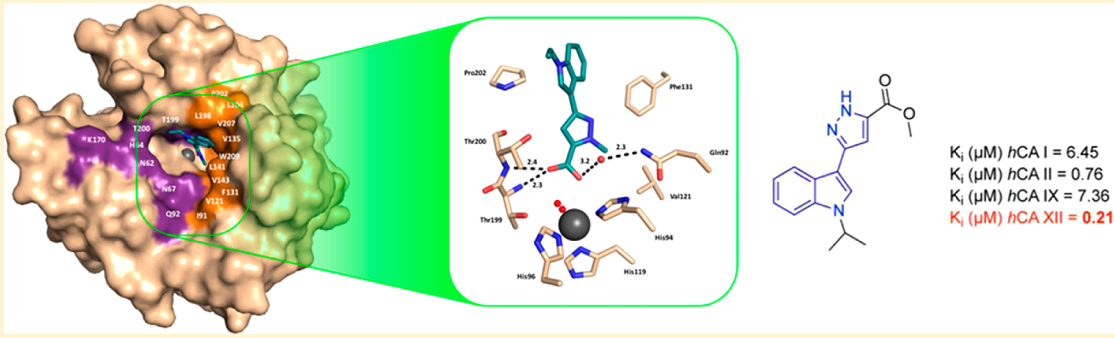

ABSTRACT: We report the synthesis, biological evaluation, and structural study of a series of substituted heteroaryl-pyrazole carboxylic acid derivatives. These compounds have been developed as inhibitors of specific isoforms of carbonic anhydrase (CA), with potential as prototypes of a new class of chemotherapeutics. Both X-ray crystallography and computational modeling provide insights into the CA inhibition mechanism. Results indicate that this chemotype produces an indirect interference with the zinc ion, thus behaving differently from other related nonclassical inhibitors. Among the tested compounds, **2c** with K_i = 0.21 μM toward *h*CA XII demonstrated significant antiproliferative activity against hypoxic tumor cell lines. Taken together, the results thus provide the basis of structural determinants for the development of novel anticancer agents.

KEYWORDS: *Carbonic anhydrase, hCA XII inhibitors, heteroaryl-pyrazole carboxylic acids, X-ray crystallography, computational docking, hypoxic tumors*

Many currently used antitumor drugs demonstrate relatively poor selectivity for cancer cells, causing frequent toxicity and side effects. A current strategy to overcome this impasse relies on the identification of biological targets that are exclusive, or at least highly prevalent, in cancer cells. One of the most suited hallmarks of cancer is metabolic reprogramming, which offers new opportunities for the development of innovative chemotherapeutics.[1] In particular, hypoxia, a common condition in tumor microenvironment, promotes consistent metabolic adaptation, such as the switching of energetic metabolism from aerobic to anaerobic glycolysis.[2,3] A critical consequence of this phenomenon is the overproduction of weak acid species, such as lactic acid. In order to preserve their acid−base homeostasis, cancer cells adopt a series of adaptive mechanisms through the activation of specific factors (such as the hypoxia-inducible factor 1, HIF-1), which promptly remove/rebalance the H^+ excess from the cells, thus lowering the extracellular pH.[4,5]

As far as other putative biological pathways involved with hypoxic cancer are concerned, carbonic anhydrases (CAs), a

Received: June 6, 2017
Accepted: July 31, 2017
Published: July 31, 2017

DOI: 10.1021/acsmedchemlett.7b00229
ACS Med. Chem. Lett. 2017, 8, 941−946

family of metalloenzymes that catalyze the biochemical reaction of carbon dioxide hydration to produce a bicarbonate ion and a proton, are emerging as potential biological targets for cancer therapy.[6] Previously, two tumor-associated extracellular transmembrane carbonic anhydrase isozymes (*h*CA IX and *h*CA XII) were identified, cloned, and sequenced.[6−8] These two CA isoforms have been shown to be expressed in a wide variety of malignancies and appear to be tightly regulated by microenvironmental hypoxia.[7,8] This phenomenon is particularly evident in highly malignant solid tumors and has been linked to poor blood perfusion that reduces the provision of oxygen and nutrients for cancer cells, thus inducing a series of adaptive responses (i.e., metabolic shift to anaerobiosis and increased amino acids catabolism) that lead to lower extracellular pH, a condition that is not favorable for cell survival.

In this scenario, the extracellular CA isoforms are implicated in rebalancing the acid/base equilibrium of the extracellular medium.[6,9,19] Specifically, *h*CA XII is minimally expressed in a variety of normal tissues including kidney, colon, prostate, pancreas, ovary, testis, lung, and brain, but its expression is upregulated in cancer cells originating from these tissues.[7] Several recent studies proposed *h*CA XII as a suitable and attractive target for both diagnostic and therapeutic intervention, particularly on the management of hypoxic tumors normally nonresponsive to classical chemo- and radiotherapies.[9−12]

Primary sulfonamides, the most clinically used CAs inhibitors (CAIs), have been shown to reverse the effect of the extracellular CAs and inhibit the growth of cancer cells in the low nanomolar or micromolar range.[13−15] However, one main drawback of these classical sulfonamide CAIs is the lack of selectivity for inhibiting transmembrane CAs over the other cytoplasmic CA isoforms present in humans and in mouse model systems. For this reason, efforts are being initiated to find novel CAIs, in order to explore molecular diversities and discover original pharmacophores and chemotypes.[13−16]

This study focuses on the structural optimization of a previously identified hit compound, the 3-(1-ethyl-1*H*-indol-3-yl)-1*H*-pyrazole-5-carboxylic acid (**1a**, Chart 1),[17] in order to generate and evaluate a new series of indolylpyrazole-5-carboxylic acids/esters with improved inhibition profile toward *h*CA IX and *h*CA XII.

Chart 1. Design and General Structure of Title Compounds

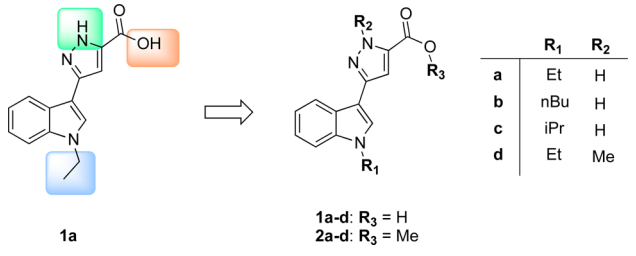

	R_1	R_2
a	Et	H
b	nBu	H
c	iPr	H
d	Et	Me

Preliminary major modifications of **1a** have been made by varying the substituents at the nitrogen atoms both on the indole and pyrazole rings and by esterification of the carboxylic functionality to generate the series **1a−d** and **2a−d** (Chart 1). Specifically, *N*-alkylation of the indole was first explored to modulate lipophilicity; second, *N*-methylation of the pyrazole was introduced to abolish N−H interaction; finally, on the basis of the assumption that the carboxylic moiety is a necessary feature for the inhibitory activity, we examined the effect of esterification on the activity.

Compounds **1a−d** and **2a−d** were synthesized starting from the 3-acetyl indole **3** by alkylation reaction with the appropriate alkyl bromide to obtain the *N*-alkyl-3-acetyl-indole derivatives **4a−c** (Scheme 1).

Scheme 1. Synthetic Route for the Preparation of Compounds 1a−d and 2a−d

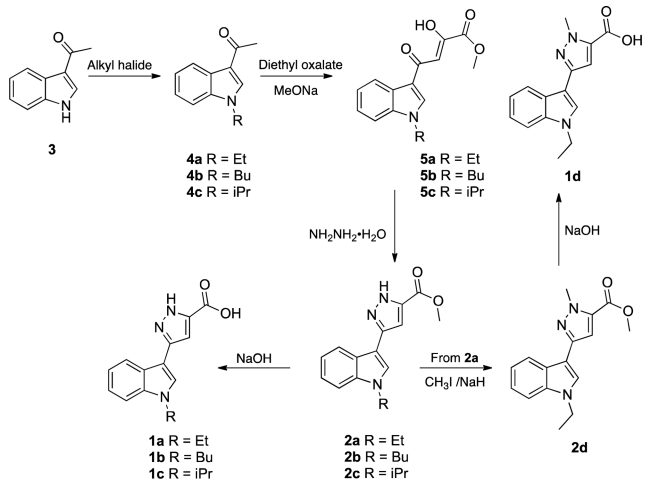

These intermediates were reacted with diethyl oxalate in the presence of sodium methoxide in MeOH, to provide the respective *β*-diketoesters **5a−c**. The latter were found to exist in the keto-enol form in DMSO since ^{1}H NMR experiments showed a singlet centered at 6.87 ppm (for **5a,b**) and at 6.89 (for **5c**) attributable to the enolic CH of the hydroxy-keto motif. Next, the compounds **5a−c** were treated with hydrazine monohydrate to generate the pyrazole derivatives **2a−c** in appreciable yields (46−93%). Then, the acids **1a−c** were obtained by alkaline hydrolysis of the esters **2a−c**. Finally, the compound **2d**, containing a methyl group on the nitrogen of pyrazole ring, was synthesized by alkylation of intermediate **2a** with iodomethane in the presence of NaH. The corresponding acid **1d** was obtained from **2d** by alkaline hydrolysis with NaOH in ethanol at reflux.

Compounds **1a−d** and **2a−d** were tested for their ability to inhibit a panel of representative isoforms of human CAs (I, II, IX, and XII, Table 1). Catalytic activities were measured by a stopped-flow technique, as previously described (see Supporting Information).

Although structural modifications of the lead compound **1a** reduced the potency and selectivity against *h*CA I isoform (work is in progress to clarify the behavior of this outlier compound), these new compounds showed an interesting selectivity toward *h*CA XII, with K_i values ranging from 0.21 to 0.57 *μ*M (Table 1). Moreover, with the exception of **1b** and **2a**, the tested compounds effectively interfere with *h*CA II catalytic activities in submicromolar/micromolar concentration range (K_i values of 0.41−6.95 *μ*M, Table 1). On the contrary, no significant inhibition or slightly weaker inhibitory action toward *h*CA I and *h*CA IX (with the exception of **2d** and **2a**, with K_i values of 0.62 and 0.47 *μ*M, for *h*CA I and *h*CA IX, respectively), were revealed.

Overall, the biological profile appeared to be substantially independent from the nature of substituents on both the indole and the pyrazole rings. However, although a proper structure−activity relationship (SAR) for *h*CA XII inhibition is not feasible at this stage, it is plausible that structural determinants

DOI: 10.1021/acsmedchemlett.7b00229
ACS Med. Chem. Lett. 2017, 8, 941−946

Table 1. Inhibition of *h*CA Isoforms I, II, IX and XII with Compounds 1a−d and 2a−d

	K_i (μM)[a]			
compd	*h*CA I[b]	*h*CA II[b]	*h*CA IX[c]	*h*CA XII[c]
1a	0.042 ± 0.0001	1820 ± 9	7.79 ± 0.06	7.78 ± 0.04
1b	5.33 ± 0.04	4.70 ± 0.01	4.51 ± 0.03	0.34 ± 0.006
1c	4.83 ± 0.07	0.70 ± 0.008	18.9 ± 0.21	0.28 ± 0.01
1d	6.61 ± 0.02	0.78 ± 0.009	2.91 ± 0.04	0.44 ± 0.005
2a	4.31 ± 0.06	6.95 ± 0.08	0.47 ± 0.003	0.57 ± 0.008
2b	5.93 ± 0.06	0.53 ± 0.003	7.90 ± 0.08	0.35 ± 0.002
2c	6.45 ± 0.03	0.76 ± 0.05	7.36 ± 0.04	0.21 ± 0.01
2d	0.62 ± 0.005	0.41 ± 0.007	3.02 ± 0.008	0.31 ± 0.01
AAZ	0.25 ± 0.01	0.012 ± 0.001	0.025 ± 0.002	0.006 ± 0.0005
MZA	0.78 ± 0.04	0.014 ± 0.001	0.027 ± 0.008	0.034 ± 0.002
DCP	1.2 ± 0.1	0.038 ± 0.003	0.050 ± 0.005	0.050 ± 0.004

[a]Errors in the range of ±5−10% of the reported value from three different determinations. [b]Full length. [c]Catalytic domain. AAZ, acetazolamide; MZA, methazolamide; DCP, dichlorophenamide.

of this chemotype (i.e., indole ring system, lypophilic substituents at the nitrogen indole, and carboxylic functionality) appear to be an optimal combination to effectively inhibit the *h*CA XII (with a certain mutual interference with cytosolic *h*CA II catalytic activity). Again, no relevant differences could be observed between acids and esters on the inhibition profile. Nevertheless, among the tested compounds, compound **2c** (K_i = 0.21 μM) proved to be the most active compound in inhibiting *h*CA XII, thus demonstrating to be one of the most effective nonsulfonamide-based inhibitors toward this CA isoform.

Since the indolylpyrazole-5-carboxylate backbone appeared to be an original chemotype for CA inhibition, the interaction of representative compound **1d** with *h*CA II was studied by X-ray crystallography and determined to 1.2 Å resolution (statistics summarized in Table S1). Structural analysis of the *h*CA II/**1d** complex indicates that the compound does not bind directly to the active site zinc(II) ion, making it dissimilar to other potent CA inhibitors.[18] For example, apart from the classical (i.e., sulfonamides and their isosteres) zinc binders and nonclassical (e.g., carboxylates, hydroxamates, dithiocarbamates, and phosphonates) CAIs, other classes of compounds were found to act through another mechanism of action by (a) anchoring to the metal ion coordinated nucleophile binding in a more distant part of the active site cavity compared with the zinc binders (phenols, polyamines, esters, sulfocoumarins), (b) occluding the entrance of the active site cavity (coumarins), and (c) binding outside the active site (benzoic acids).[18]

Instead, the compound **1d** utilizes a carboxylic acid moiety to substitute the typical location of a zinc-binding group (ZBG).[19,20]

As such, the compound resides buried in the *h*CA II active site and interacts with adjacent residues to the catalytic zinc. This mode of binding results in the observation of a disordered water molecule coordinated to the active site zinc (Figure 1). However, compound **1d** displaces the ordered water network in the active site that has been shown to be important for catalysis. Key interactions are observed between the carbonyl oxygen of compound **1d** and the backbone NH of both Thr199 and Thr200 (2.3 and 2.4 Å, respectively). The carbonyl hydroxyl also forms a hydrogen bond with a coordinated solvent molecule within the active site (bond distance = 3.2 Å), which is then stabilized by a hydrogen bond with the amide of Gln92 (bond distance = 2.3 Å). Compound **1d** also displays extensive interactions with the hydrophobic pocket of the *h*CA II active site. Specifically, van der Waals interactions with residues Val121, Phe131, and Pro202 of the enzymes hydrophobic pocket are predicted to stabilize the "tail" region of compound **1d** and are therefore suggested to greatly stabilize the enzyme/inhibitor complex (Figure 2).

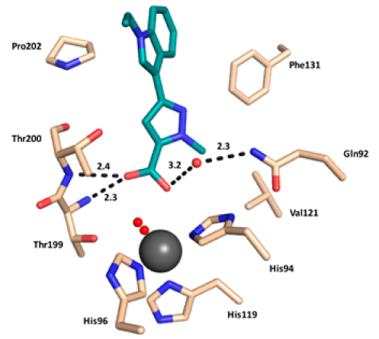

Figure 1. *h*CA II (light brown) in complex with compound **1d** (deep teal). Hydrogen bond interactions are shown with distances (Å) and amino acids labeled. Water molecules are depicted as red spheres. Zinc ion is represented as a gray sphere. This chemotype binds with residues located in proximity of the catalytic site, which displaces the ordered water network, thus definitely producing an indirect interference with the zinc ion.

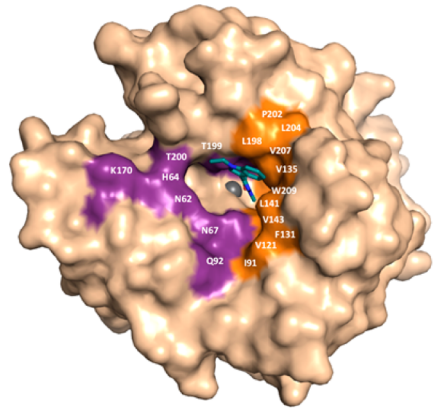

Figure 2. Surface representation showing the location of compound **1d** (deep teal) in the *h*CA II active site (light brown). Hydrophobic (orange) and hydrophilic (purple) residues are highlighted and relative locations labeled.

DOI: 10.1021/acsmedchemlett.7b00229
ACS Med. Chem. Lett. 2017, 8, 941−946

In order to investigate the interation of the other compounds **1a−c** and **2a−d** within the catalytic sites of *h*CA II (new PDB code: 5CJL) and *h*CA XII (PDB code: IJCZ), a series of docking studies was performed. Preliminarily, we envisaged that in the assembly of ligand−target complex, water molecules could play a crucial role in careful calculations. To be able to accomplish the calculation with manageable computational complexity, the docking procedure recently proposed by Olson and Forli[21] was employed. This procedure allows the effect of water molecules located in proximity of ligands to be considered. This method entails the use of a monatomic pseudoatom (W) as a surrogate of the water molecule. First, compound **1d** was docked into the X-ray crystal structure, obtaining the same binding mode as in the X-ray crystallography, within the experimental resolution limits (Figure S1A). This established the robustness of the method, and then **1d** was also modeled with CA XII (Figure S1B).

After this, the docking settings were optimized, and docking runs were performed for all remaining ligands (i.e., **1a−c** and **2a−d**) in the active sites of *h*CA II and XII isoforms. Graphical representations of top-ranking binding modes obtained for these ligands are shown in Figures S2A,B, S3, and S4.

From the structural point of view, *h*CA II and XII exhibit considerable tertiary structure similarity, with an rmsd value of 1.2 Å; some discrepancies are present on the surface of proteins in concomitance of random coiled regions (Figure S5). Moreover, only three residues exhibited a rmsd greater than 3 Å. Focusing on the catalytic region, the primary sequence appears highly conserved, with the exception of nine residues (i.e., A65S, N67K, E69D, I91T, P131A, G132S, V135S, Q136N, and L204N, indicated as Res_{CAII}-number-Res_{CAXII}). As shown in Table S2, 18 and 22 residues, for *h*CA II and XII, respectively, stabilize the ligand−protein complex. Moreover, the residues at positions 94, 131, 135, 198, 200, and 202, were also involved in ligand interaction. Furthermore, the key residue Thr199 is predicted to establish an interaction only for *h*CA II, whereas residues in positions 91, 92, 96, and 141 are predominantly involved in contacts with *h*CA XII active site. Although differences were found between the binding modes of ligands to the same CA isoform, a similar orientation pattern and disposition within the catalytic site were observed. In the case of the *h*CA II, all ligands accommodated almost perpendicularly to the plane of the three coordinating histidines with the carboxylate group directed toward the zinc-bound water. In the case of *h*CA XII, ligands are in a decentered position with the scaffold lying along the protein wall formed by residues Gln92 and His94. This particular arrangement implies that the carboxylate group makes contact with the deep-water from the lateral side. In all cases (with the exception of the less active compound **1a**), it allows the formation of a hydrogen bond with the imidazole ring of His96. Regarding the most active compound **2c** against *h*CA XII, docking results showed that the most favorable binding conformation with *h*CA II is superimposable to that of compound **1d** obtained experimentally by X-ray crystallography (Figures S1A and 3A).

Both compounds shared common residue interactions (Table S2), with slight differences for the absence of a hydrophobic contact with Val121 (for **2c**), due to the lacking *N*-methyl group in position 1 of pyrazole ring and the presence of a methoxy group receptor that is able to establish additional contact with Trp209. It is worth noting that, when docked in *h*CA XII catalytic site, compound **2c** appeared located inside a binding pocket formed by 13 residues (Figure 3B and Table S2), with the presence of three strong hydrogen bonds with His96 and Thr200. An additional observation could be made about the comparison of the inhibition values between **2a** and **2d**. Although compound **2a** is not the most potent compound toward *h*CA XII, it exhibits a significant selectivity profile transmembrane vs cytosolic isoforms (i.e., *h*CA XII/hCA II), which resulted about 10-fold higher (as ratio of selectivity indexes) than that of **2d** (K_i *h*CA XII/K_i hCA II = 12.2 and 1.3, for **2a** and **2d**, respectively, Table 1). Considering that the only structural difference of **2a** with respect to compound **2d** is the *N*-methylation of the pyrazole ring, this modification might be relevant for selectivity. Analyses of postdocking energies such as estimated free energy of binding and related estimated inhibition constant (E.I.C.) values, calculated for each compound (i.e., E.I.C. = 83.29 and 34.42 μM, against *h*CA II, and 5.38 and 6.60 μM, against *h*CA XII, for **2a** and **2d**, respectively), seem to support this behavior.

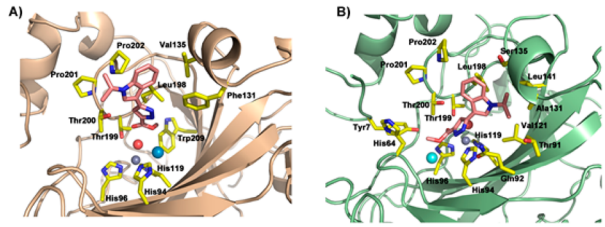

Figure 3. Predicted binding modes for the most promising compound **2c** within the catalytic pockets of *h*CA II (A) and XII (B) isoforms. *h*CA II and XII are colored as light brown and pale green, respectively; side chain of significant residues are represented as yellow sticks and labeled. Ligand **2a** is in pink sticks. Zinc cofactor, zinc-bound water, and pseudoatoms are depicted as spheres and colored in gray, red, and pale blue or cyan, respectively.

The inhibitory effect of the compounds **1a**, **2a**, **1c**, and **2c** on CA activity (particularly of *h*CA IX and/or XII) was evaluated in terms of cell viability of three human cancer cell lines (hormone-independent prostate cells, PC-3; human embryonic kidney, HEK 293 cells; human neuroblastoma cells, SH-SY5Y). First, HEK 293 cells were treated for 24 h with increasing concentrations of **1a**, **2a**, **1c**, and **2c** (Figure S6A). No significant antiproliferative effect was detected at the 1, 10, 30, or 100 μM of compound treatment, with the exception of **2c**, which exhibited a dose-dependent cell growth inhibition reaching roughly the 70% antiproliferative effect at the highest concentration. Better results were found when the compounds were tested on PC-3 cells at the same conditions (Figure S6B) as well as on SH-SY5Y cell lines after 48 h of treatment (~85 growth inhibition, Figure S6C).

Since hypoxia-induced upregulation of *h*CA IX and XII are key components of the complex response of cancer cells to the evolving low oxygen environment, compound **2c** was further investigated for its antiproliferative potency on neuroblastoma SH-SY5Y cells in normal and in simulated hypoxic conditions using cobalt(II) chloride (Figure 4).[22] As expected, the addition of cobalt(II) chloride, a known chemical inducer of hypoxia-inducible factors, significantly increased the susceptibility of the cells to the **2c** treatment, showing a 40% reduction of cell viability at an inhibitor concentration of 30 μM ($p < 0.05$ vs untreated cells).

A new series of compounds bearing a 3-(1*H*-indol-3-yl)pyrazole-5-carboxylic acid scaffold have been synthesized and evaluated for their selective inhibition of *h*CA XII. Among the tested compounds, **2c** (K_i = 0.21 μM) resulted the most

DOI: 10.1021/acsmedchemlett.7b00229
ACS Med. Chem. Lett. 2017, 8, 941−946

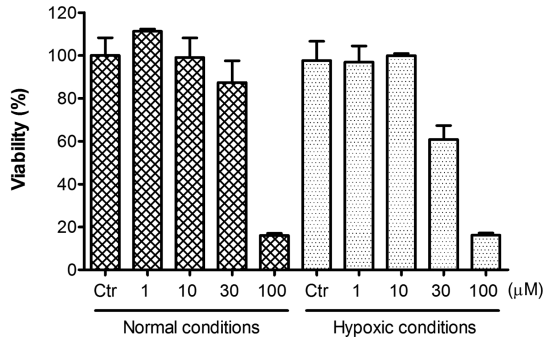

Figure 4. Dose-dependent antiproliferative activity of compound **2c** on human neuronal SH-SY5Y cells (measured by percentage of cell viability after 48 h of treatment) assessed in normal and simulated hypoxic conditions.

potent *h*CA XII inhibitor and exhibited cytotoxicity toward three different cancer cell lines. Interestingly, this chemotype behaves differently from other related nonclassical inhibitors. In fact, it does not directly bind to the metal ion or to the zinc-bound water/hydroxide ion: the zinc ion−carboxylate distances in our model are ∼3.78 and ∼4.62 Å (for contact with each oxygen atom), too much longer to support a favorable zinc ion coordination to carboxylate functionality of the ligand. Otherwise, this compound seems to establish contacts with residues located in proximity of the catalytic site, which displaces the ordered water network (shorter zinc ion−water distance, i.e., 2.26 and 1.94 Å, for zinc−O1 and zinc−O2, was revealed), thus definitively producing an indirect interference with the zinc ion. However, **2c** displayed improved antiproliferative effects when tested in simulated hypoxia conditions, considering the putative expected involvement of *h*CA XII inhibition. These results could provide structural determinants for the discovery of novel anticancer agents with original mechanism of action, warranting further development.

■ ASSOCIATED CONTENT

Supporting Information

The Supporting Information is available free of charge on the ACS Publications website at DOI: 10.1021/acsmedchemlett.7b00229.

Experimental details for chemistry, X-ray crystallography, and molecular modeling. ^{1}H NMR spectra for title compounds **1b−d** and **2a−d**, and their intermediates **4a−c** and **5a−c**. Mass spectra for **1b−d**, **2a−d**, and **5a−c**. X-ray crystallography statistics for data processing and refinement of **4d** in complex with *h*CA II. Details of experimental biology procedure. Additional molecular modeling data. Antiproliferative activity of compounds **1a**, **2a**, **1c**, and **2c** (PDF)

■ AUTHOR INFORMATION

Corresponding Authors

*(M.S.) Phone: +39 079-228-753. Fax: +39 079-229-559. E-mail: mario.sechi@uniss.it.

*(C.T.S.) Phone: 39-055-4573005. Fax: +39-055-4573385. E-mail: claudiu.supuran@unifi.it.

ORCID

Mauro Carcelli: 0000-0001-5888-4556

Dominga Rogolino: 0000-0003-2295-5783

Vanna Sanna: 0000-0001-9068-6349

Claudiu T. Supuran: 0000-0003-4262-0323

Mario Sechi: 0000-0003-2983-6090

Author Contributions

[∇]These authors contributed equally to this work. The manuscript was written through contributions of all authors. All authors have given approval to the final version of the manuscript.

Notes

The authors declare no competing financial interest.

PDB ID 5CJL: **1d** in complex with *h*CA II (Table S1).

The content is solely the responsibility of the authors and does not necessarily represent the official views of the National Institutes of Health.

■ ACKNOWLEDGMENTS

This research was financed in part the National Institutes of Health, project CA165284. C.L. is supported by the National Center for Advancing Translational Sciences of the National Institutes of Health under University of Florida Clinical and Translational Science Awards TL1TR001428 and UL1TR001427. We would also like to acknowledge the staff at Cornell High Energy Synchrotron Source (CHESS) for assisting with X-ray data collection.

■ ABBREVIATIONS

hCA, human carbonic anhydrase; CAIs, carbonic anhydrase inhibitors; K_i, inhibition constant; ZBG, zinc-binding group; PC-3, hormone-independent prostate cells; HEK 293, human embryonic kidney cells; SH-SY5Y, human neuroblastoma cells

■ REFERENCES

(1) Hanahan, D.; Weinberg, R. A. Hallmarks of cancer: the next generation. *Cell* **2011**, *144*, 646−674.

(2) Gatenby, R. A.; Gillies, R. J. Why do cancers have high aerobic glycolysis? *Nat. Rev. Cancer* **2004**, *4*, 891−899.

(3) Gilkes, D. M.; Semenza, G. L.; Wirtz, D. Hypoxia and the extracellular matrix: drivers of tumour metastasis. *Nat. Rev. Cancer* **2014**, *14*, 430−439.

(4) Semenza, G. L. Oxygen sensing, hypoxia-inducible factors, and disease pathophysiology. *Annu. Rev. Pathol.: Mech. Dis.* **2014**, *9*, 47−71.

(5) Chiche, J.; Brahimi-Horn, M. C.; Pouysségur, J. Tumour hypoxia induces a metabolic shift causing acidosis: a common feature in cancer. *J. Cell. Mol. Med.* **2010**, *14*, 771−794.

(6) Neri, D.; Supuran, C. T. Interfering with pH regulation in tumours as a therapeutic strategy. *Nat. Rev. Drug Discovery* **2011**, *10*, 767.

(7) Kallio, H.; Rodriguez Martinez, A.; Hilvo, M.; Hyrskyluoto, A.; Parkkila, S. Cancer-associated carbonic anhydrases IX and XII: effect of growth factors on gene expression in human cancer cell lines. *J. Cancer Mol.* **2010**, *5*, 73−78.

(8) Wykoff, C. C.; Beasley, N. J. P.; Watson, P. H.; Turner, K. J.; Pastorek, J.; Sibtain, A.; Wilson, G. D.; Turley, H.; Talks, K. L.; Maxwell, P. H.; Pugh, C. W.; Ratcliffe, P. J.; Harris, A. L. Hypoxia-inducible expression of tumor-associated carbonic anhydrases. *Cancer Res.* **2000**, *60*, 7075−7083.

(9) Pastorekova, S.; Zatovicova, M.; Pastorek, J. Cancer-associated carbonic anhydrases and their inhibition. *Curr. Pharm. Des.* **2008**, *14*, 685−698.

(10) Parkkila, S. Significance of pH regulation and carbonic anhydrases in tumour progression and implications for diagnostic and therapeutic approaches. *BJU Int.* **2008**, *101* (Suppl. 4), 16−21.

(11) Chiche, J.; Ilc, K.; Laferrière, J.; Trottier, E.; Dayan, F.; Mazure, N. M.; Brahimi-Horn, M. C.; Pouysségur, J. Hypoxia-inducible carbonic anhydrase IX and XII promote tumor cell growth by

DOI: 10.1021/acsmedchemlett.7b00229
ACS Med. Chem. Lett. 2017, 8, 941−946

counteracting acidosis through the regulation of the intracellular pH. *Cancer Res.* **2009**, *69*, 358−368.
(12) Ivanov, S.; Liao, S. Y.; Ivanova, A.; Danilkovitch-Miagkova, A.; Tarasova, N.; Weirich, G.; Merrill, M. J.; Proescholdt, M. A.; Oldfield, E. H.; Lee, J.; Zavada, J.; Waheed, A.; Sly, W.; Lerman, M. I.; Stanbridge, E. J. Expression of hypoxia-inducible cell-surface transmembrane carbonic anhydrases in human cancer. *Am. J. Pathol.* **2001**, *158*, 905−919.
(13) Supuran, C. T. Carbonic anhydrases: novel therapeutic applications for inhibitors and activators. *Nat. Rev. Drug Discovery* **2008**, *7*, 168−181.
(14) Supuran, C. T. *Drug Design of Zinc-Enzyme Inhibitors: Functional, Structural, and Disease Applications, Part II*; Wiley: Hoboken, NJ, 2009.
(15) Supuran, C. T., Scozzafava, A., Conway, J., Eds. *Carbonic Anhydrase: Its Inhibitors and Activators*; CRC Press: Boca Raton, FL, 2004.
(16) Alterio, V.; Di Fiore, A.; D'Ambrosio, K.; Supuran, C. T.; De Simone, G. Multiple binding modes of inhibitors to carbonic anhydrases: how to design specific drugs targeting 15 different isoforms? *Chem. Rev.* **2012**, *112*, 4421−4468.
(17) Sechi, M.; Innocenti, A.; Pala, N.; Rogolino, D.; Carcelli, M.; Scozzafava, A.; Supuran, C. T. Inhibition of α-class cytosolic human carbonic anhydrases I, II, IX and XII, and β-class fungal enzymes by carboxylic acids and their derivatives: New isoform-I selective nanomolar inhibitors. *Bioorg. Med. Chem. Lett.* **2012**, *22*, 5801−5806.
(18) Supuran, C. T. How many carbonic anhydrase inhibition mechanisms exist? *J. Enzyme Inhib. Med. Chem.* **2016**, *31*, 345−360.
(19) Lomelino, C. L.; Supuran, C. T.; McKenna, R. Non-classical inhibition of carbonic anhydrase. *Int. J. Mol. Sci.* **2016**, *17*, 1150.
(20) Langella, E.; D'Ambrosio, K.; D'Ascenzio, M.; Carradori, S.; Monti, S. M.; Supuran, C. T.; De Simone, G. A combined crystallographic and theoretical study explains the capability of carboxylic acids to adopt multiple binding modes in the active site of carbonic anhydrases. *Chem. - Eur. J.* **2016**, *22*, 97−100.
(21) Forli, S.; Olson, A. J. A force field with discrete displaceable waters and desolvation entropy for hydrated ligand docking. *J. Med. Chem.* **2012**, *55*, 623−638.
(22) Al Okail, M. S. Cobalt chloride, a chemical inducer of hypoxia-inducible factor-1α in U251 human glioblastoma cell line. *J. Saudi Chem. Soc.* **2010**, *14*, 197−201.

DOI: 10.1021/acsmedchemlett.7b00229
ACS Med. Chem. Lett. 2017, 8, 941−946